AD A030769

SETEC-MME-76-030

12

Technical Report

EFFECTS OF SOLUTE REDISTRIBUTION ON THE STRUCTURE AND PROPERTIES OF CAST ALLOYS

August 1976

CONTRACT N00014-75-C-0800

OFFICE OF NAVAL RESEARCH
METALLURGY BRANCH

DDC
RECEIVED
OCT 14 1976
D

by

J. Mathew, S. A. David, K. Y. Lin, and H. D. Brody

DEPARTMENT OF METALLURGICAL AND MATERIALS ENGINEERING
UNIVERSITY OF PITTSBURGH

DISTRIBUTION STATEMENT
Approved for public release;
Distribution Unlimited

ACCESSION for
NTIS White Section
DDC Buff Section

(14) SETEC-MME-76-030

(9) Technical Report.

A

(6) EFFECTS OF SOLUTE REDISTRIBUTION ON THE STRUCTURE AND PROPERTIES OF CAST ALLOYS.

(11) Aug[redacted]76 (12) 34p.

(15) CONTRACT N0014-75-C-0800

OFFICE OF NAVAL RESEARCH
METALLURGY BRANCH

by

(10) J. Mathew, S. A. David, K. Y. Lin and H. D. Brody

DEPARTMENT OF METALLURGICAL AND MATERIALS ENGINEERING
UNIVERSITY OF PITTSBURGH

DDC
RECEIVED
OCT 14 1976

DISTRIBUTION STATEMENT A
Approved for Public Release;
Distribution Unlimited

402241

Technical Report

EFFECTS OF SOLUTE REDISTRIBUTION ON THE STRUCTURE AND PROPERTIES OF CAST ALLOYS

by

J. Mathew, S. A. David, K. Y. Lin, and H. D. Brody
Department of Metallurgical and Materials Engineering
University of Pittsburgh

ABSTRACT

This report summarizes work on composite and alloy solidification presently conducted under the ONR contract and includes two papers on the simulation of heat flow and thermal stresses in continuous casting presented at the "Conference on Computer Simulation for Materials Applications" in Gaithersburg, Md. in April 1976.

A finite element analysis of heat transfer in continuous casting is presented in the first paper. The steady state conditions of the solidification of a cylindrical alloy ingot are simulated. The analysis takes into account both radial and axial heat conduction and the variation of alloy properties with temperature. The analysis has the versatility to simulate any casting configuration as the program has the capability to treat any arbitrary boundary conditions. In the mold region, where an air gap generally forms, the position of gap formation, the size of the gap and the heat transfer through the gap by conduction and radiation are computed. Values predicted by the model are in close agreement with published laboratory and industrial data.

The second paper presents a three dimensional analysis of steady state thermal stresses developed in the continuous casting of cylindrical sections. The analysis takes into account the elastic, plastic and steady state creep deformations of the castings. It can take into account virtually all boundary conditions encountered in continuous casting (friction in the mold, metallostatic head, etc.) and is applicable to both ferrous and nonferrous continuous casting. The results from the analysis are compared to the published residual stress measurements made on aluminum-12% silicon alloy (A132). The model is very useful in understanding the influence of the operating parameters on the hot tearing and cold cracking of continuous castings.

Contract N00014-75-C-0800
Office of Naval Research
Metallurgy Branch

SUMMARY OF WORK

The research supported under this ONR contract has concentrated on two overlying technological themes:

> Control of structure, microsegregation, and macrosegregation in ingots and castings by control of solidification parameters.
>
> Development of high temperature, high strength composite materials by solidification techniques.

Work on melt grown composite materials has been with eutectic and peritectic alloys. A continuing theme in eutectics has been establishing the relation between growth conditions in zone melting and microstructure for Pb-Sn, a low temperature model system, and Nb-Nb_2C, a high temperature model system. Present work in this area deals with defining changes in the microstructure that occur immediately behind the growth interface in Nb-Nb_2C and determining whether there is a plate to rod change in morphology with growth rate in Pb-Sn. Such a transition in morphology with growth rate has been demonstrated for Nb-Nb_2C.

Studies on the high temperature properties of Nb-Nb_2C have been undetaken with the aim of defining the effect of microstructural variables on the properties, thermal stability and creep resistance. Nb-Nb_2C composite samples with plate and rod-like carbide morphologies showed good microstructural stability when exposed to temperatures up to 1125^{o}C. On exposure of these samples to temperatures in excess of one half the eutectic temperature, the structures coarsen appreciably. For samples with plate carbide morphology, the plate morphology and high aspect ratio is maintained. For samples with rod-like carbide morphology, the major change was a reduction in the total number of carbide fibers and a transition in carbide morphology from rods to

plates. Present optical and S.E.M. observations indicate the change in morphology on annealing is a two dimensional coarsening with preferential growth of the surviving carbide rods on the (100) faces until they merge to form plates.

Emphasis in the creep work has been placed on relating the microstructure of eutectic Nb-Nb_2C composites to their creep properties. It is worth noting that the steady state creep rate at 1100°C of well aligned Nb-Nb_2C composites is the order of the creep rate of Ni-base superalloys at 800°C. There is a very strong dependence of creep rate on structure. The creep rate can increase by two orders of magnitude in going from a well aligned composite structure to a well aligned dendritic structure. Misorientation and banding have a major influence on creep rate. The stress exponent varies from 3 to 14 depending on microstructure. The dependence of activation energy on microstructure (if any) is being measured. The metallographic investigation of samples after creep testing is underway.

The first work on peritectic alloys, the Pb-Bi system, brought surprising results. Aligned two phase composite structures were produced and these were assumed to be the result of dendritic growth at high degrees of undercooling. It was also possible to produce single phase supersaturated solutions in compositions that, at equilibrium, should be a two phase, peritectic mixture. We have now confirmed the results for Sn-Cd. New work will be on higher temperature peritectic systems.

The work on producing an oxide dispersion strengthened alloy by casting has met with mixed results. We have been able to rheocast vacuum melted alloys and to mix in very fine oxide dispersions. However, we have not been able to mix and cast sufficiently quickly to avoid reaction between the oxide and solute in the melt. Proposed work would be small scale experiments to measure the effect of surface treatment and other particle variables in delaying the reaction.

A computer program has been developed to simulate the steady state continuous casting of round ingots. The program calculates temperature distributions throughout the ingot and build up of thermal stresses as a function of casting variables and alloy properties. Presently, parametric studies are being simulated to see the individual and combined effects of the variables. The next sections of this report deal with the analysis method of the continuous casting simulaton.

The remaining alloy work deals with titanium and NITINOL. The titanium work will evaluate the tendency of these alloys to exhibit macrosegregation as a result of the bulk movement of enriched liquid. The NITINOL work will first aim at developing a predictive ability with regard to manufacturing process and transition range and second will be to prepare a modest inventory of research materials.

COMPUTER SIMULATION OF CONTINUOUS CASTING

Much of the basic work we have carried out under this contract is applicable to directional solidification processes; that is, casting methods wherein there is a positive temperature gradient in the liquid ahead of the dendrite tips. Continuous casting, electroslag remelting, and vacuum arc remelting are examples of directional solidification processes. A comprehensive engineering model of these processes would include being able to predict heat flow patterns, fluid flow patterns, states of stress, grain and dendrite structure, micro- and macrosegregation, inclusion shapes and distributions, hot carcking, and residual stresses. One aspect for which we have developed a model is the build up of thermal stresses in continuous casting.

The numerical simulation of continuous casting has been developed by J. Mathew for his Ph.D. thesis. The simulation utilizes the finite element method and considers the steady state portion of the casting of round ingots. In order to make the thermal stress analysis of continuous casting, it is

prerequisite that analysis be made of the steady state temperature distribution in the various regions of the ingot and certain properties of the alloy being studied be available as functions of temperature. The important parameters include phase relations, stiffness, relaxation characteristics, thermal expansion coefficient, yield strength, and solidification characteristics. In order to make the simulation appropriate nonferrous as well as ferrous casting, both radial and axial heat transfer are taken into account, i.e., the heat flow analysis is two dimensional. The stress analysis is three dimensional and has the capability of accounting for elastic, plastic, and creep strains. The inclusion of creep behavior in the simulation reflects our feeling that the build up of thermal stresses is strongly dependent on time and rate. The details of the analysis are covered in the papers included with this report.

Presently, the program is being applied to parametric studies of the effect of casting variables and alloy variables on the thermal pattern and the build up of thermal stresses in continuous casting. The casting parameters being considered are section size, mold length, cooling sequence and intensities, casting rate, casting superheat, and pressure head. The program is also being applied to several actual cases where alloy and casting data are available. As is covered in the papers, the results of the program are in good agreement with available published data. Another aspect of the present effort is the documentation of the program to the state it can be widely used.

The present program has been built in modular fashion so that in subsequent phases of the development we will be able to use the existing program as a framework for simulating the vertical casting of slabs and the influence of perturbations in casting conditions.

Presented at Conference on Computer Simulation for Materials Applications,
Gaithersburg, MD, April 1976.

ANALYSIS OF HEAT TRANSFER IN CONTINUOUS CASTING USING A FINITE ELEMENT METHOD

J. Mathew and H. D. Brody
Metallurgical and Materials Engineering
University of Pittsburgh

Abstract

A finite element analysis of heat transfer in continuous casting is presented. The steady state conditions of the solidification of a cylindrical alloy ingot are simulated. The analysis takes into account both radial and axial heat conduction and the variation of alloy properties with temperature. The analysis has the versatility to simulate any casting configuration as the program has the capability to treat any arbitrary boundary conditions. In the mold region, where an air gap generally forms, the position of gap formation, the size of the gap and the heat transfer through the gap by conduction and radiation are computed. Values predicted by the model are in close agreement with published laboratory and industrial data.

Introduction

This paper presents part of a simulation program (PCCTSS-Pitt Simulation) developed at the University of Pittsburgh to study the continuous casting process. This paper describes the heat transfer analysis. An accompanying paper (1) describes how the data from the heat transfer analysis can be used to compute the three dimensional stresses and strains in the casting. The two simulations are intended to provide a valuable tool for the study and design of cylindrical continuous casting processes.

The present thermal analysis is developed so that it can simulate both ferrous and nonferrous continuous casting. In Aluminum D.C. casting, the high conductivity of the material and the relatively slow cooling speeds employed make the axial heat transfer relatively important. In ferrous continuous casting, axial heat transfer may be neglected except for the mold exit region where the increased radial resistance to heat flow caused by the air gap formation make the axial heat transfer relatively important. None of the published analyses of heat transfer in continuous casting to this date (2-15, 17-21) (except for reference 15) takes into account the axial heat transfer in the casting. The analysis presented here accounts for the axial and radial heat transfer in the cylindrical section, the variation of thermophysical properties of the material with temperature, and the air gap formation in the casting. In the air gap, heat transfer

due to conduction and radiation are considered. The coupling effect of the air gap formed and the heat transfer are simulated by resorting to an iterative scheme. The versatility of the finite element method used in this analysis enables the use of any arbitrary boundary condition anywhere in the casting.

The previous investigations of heat transfer in continuous casting may be described under (a) analytical and empirical methods (3-7) (b) integral profile method (8-15) and (c) numerical (finite difference) methods (13,16-21). The empirical methods are very limited in scope of application. The integral profile methods are very simple to use and give fairly good results when applied to the continuous casting of steel. However, the integral profile methods do not account for the heat transfer in the axial direction in the casting or for the variation of thermophysical properties of the material with temperature. The finite difference methods are very powerful and have been shown to give reliable results when applied to the continuous casting of ferrous and nonferrous metals.

The present analysis employs the finite element method for the simulation of heat transfer in continuous casting. In this method, the casting is represented by a system of triangular ring elements. An approximate solution for the temperature field is assumed within each element and the heat flux equilibrium equations are developed at a discrete number of points within the elements. These equations are assembled and solved for the temperature distribution within the casting. This method is general and is shown to be applicable to a wide variety of problems (22). The finite element heat transfer analysis presented here has all the advantages of the implicit finite difference methods. The program is completely automated and can treat any arbitrary boundary condition. Since the finite element method is applicable to heat transfer analysis, fluid flow, diffusion or stress analysis, some of the standard structural programs can be used in the analysis of heat transfer. Also, the results from the analysis are compatible as input to a finite element stress analysis program (1). When properly formulated, the finite element method gives rise to a sparse matrix which can be solved very efficiently (PCCTSS-thermal program uses only about 1 to 3 minutes of computer time on the Pitt DEC system). Also, the accuracy of solution can be improved by increasing the number of elements or by increasing the number of nodes per element.

In this paper, the application of the finite element method to the heat transfer analysis in continuous casting is outlined. The treatment of various boundary conditions are explained. The results from the analysis are compared to the published data on heat transfer in continuous casting.

Finite Element Analysis

The steps involved in the finite element heat transfer analysis are the following:

1.) idealisation of the casting
2.) derivation of the element stiffness matrix by transforming the governing partial differential equation
3.) assembly of equations and application of proper boundary conditions
4.) solution of equations for nodal temperatures
5.) computation of the relevant quantities like freezing front location, heat flux, etc.

Each of these steps will be briefly described in the following paragraphs.

Idealisation of the Casting

The cylindrical ingot is divided into a number of triangular ring elements as shown in Figure 1. Two of these triangular ring elements grouped together give the quadrilateral ring element which is the basic element used in the present analysis. An element is defined by the nodes (e.g., i, j, k in Figure 1b) and nodal temperatures. The casting is considered to be axisymmetric and hence temperature along any of the circular nodes is constant.

Derivation of the Element Stiffness Matrix

The temperature field within a triangular element may be expressed in terms of the nodal temperatures by means of suitable interpolation functions.

$$T = N_i T_i + N_j T_j + N_k T_k = \{N_i\}\{T_i\} \quad (1)$$

where $\{N_i\}$ is the interpolation function and $\{T_i\}$ is the column matrix of nodal temperatures. The differential equation for the heat flow in continuous casting (axisymmetric) is given by

$$\nabla k \nabla T - v \rho C_p \frac{\partial T}{\partial Z} = \rho C_p \frac{\partial T}{\partial \theta} \quad (2)$$

where k is the thermal conductivity, v is the casting rate, ρ is the density, C_p is the specific heat, and θ is the time. The coordinate system is regarded as fixed with respect to the caster and the second term on the left of equation (2) accounts for heat transfer by mass flow. For steady state conditions, $\frac{\partial T}{\partial \theta} = 0$ and equation (2) reduces to

$$\nabla k \nabla T - v \rho C_p \frac{\partial T}{\partial Z} = 0 \quad (3)$$

The general boundary conditions encountered in continuous casting are

$$T = T_s \text{ (temperature specified)} \quad (4)$$

$$k \frac{\partial T}{\partial n} + q + hT = 0 \quad (5)$$

(heat flux or convection)

$$k \frac{\partial T}{\partial n} + \sigma \varepsilon (T^4 - T_\infty^4) = 0 \quad (6)$$

(radiation)

where n is the normal to the surface, T_s is the specified surface temperature, q is the heat flux from the boundary, h is the heat transfer coefficient, σ is the Stefan

Boltzmann constant, ε is the emissivity of the material, and T_∞ is the ambient temperature. Applying the Galerkin weighted residual method to equation (3) gives

$$\int_V N_i \left(\nabla k \nabla T - \nu \rho C_p \frac{\partial T}{\partial Z}\right) dV = 0 \tag{7}$$

where $dV = 2\pi r\, dr\, dZ$

$$\nabla k \nabla T = \frac{1}{r}\left(\frac{\partial}{\partial r}\left(kr\frac{\partial T}{\partial r}\right) + \frac{\partial}{\partial Z}\left(kr\frac{\partial T}{\partial Z}\right)\right) \tag{8}$$

Substituting the above into equation (7) and integrating by parts yields

$$2\pi r \int_V \left[k\frac{\partial T}{\partial r}\frac{\partial N_i}{\partial r} + k\frac{\partial T}{\partial Z}\frac{\partial N_i}{\partial Z} + \nu\rho C_p N_i \frac{\partial T}{\partial Z}\right] dr\,dZ - \int_S \left[k\frac{\partial T}{\partial r} l_r N_i + k\frac{\partial T}{\partial Z} l_Z N_i\right] dS = 0 \tag{9}$$

where l_r and l_Z are the direction cosines of the outward normal to the surface and dS is the differential surface element.

In assembling these for the entire casting, the surface integrals will cancel on neighboring elements and hence will give a contribution only for the elements which have an external surface. These then provide a convenient way of defining the boundary condition. Equations (4) through (6) can be used to specify the boundary contribution. For example, a convection boundary becomes

$$k\frac{\partial T}{\partial n} + h(T - T_\infty) = 0$$

Using the weighted residual method this transforms to

$$\int_S \left[k\frac{\partial T}{\partial n} N_i\, dS + h(T - T_\infty) N_i\, dS\right] = 0$$

and rewriting

$$\int_S \left[k\frac{\partial T}{\partial r} l_r N_i\, dS + k\frac{\partial T}{\partial Z} l_Z N_i\, dS\right] = -\int_S h(T - T_\infty) N_i\, dS \tag{10}$$

Equation (10) can be substituted into equation (9) for the element having an external surface subject to convection. Heat flux or radiation boundary conditions can be treated in a similar manner.

Substituting equation (1) to equation (9) and rearranging terms yields

$$[h]\{T_i\} = \{q\} \tag{11}$$

where $[h]$ is the element thermal stiffness matrix, $\{T_i\}$ is the nodal temperatures, and $\{q\}$ is the thermal force vector (contribution from boundary conditions).

Assembly and Solution of Equations

For each of the elements in the body a set of equations similar to (11) can be written. A number of elements may share one node and the temperature of the node should be unique. This condition is satisfied by assembling all the equations into a global equation. Assembly yields the set of equations

$$[H]\{\theta\} = \{Q\} \tag{12}$$

where $[H]$ is the global thermal stiffness matrix, $\{\theta\}$ is the vector of all nodal temperatures in the body and $\{Q\}$ is the thermal load vector (contributions from all

boundaries). Since both [H] and [Q] are known, equation (12) may be solved to get the nodal temperatures. The solutions may be done by any of the standard methods like matrix inversion methods, Gaussian elimination method or iteration methods like Gauss-Seidal method. Matrix inversion methods consume considerable computer time when a large number of equations are to be solved. Gaussian elimination methods give an exact solution except for roundoff errors. In the present analysis, the Gauss-Seidal iteration method is used. This avoids the problem of accumulation of roundoff errors and converges quickly. To conserve the use of computer memory, a sparse matrix method is used storing only the nonzero terms. The stiffness matrix obtained here is nonsymmetric (unlike most of the structural cases where the matrix is symmetric) and hence the standard solution schemes for solving symmetric matrices cannot be used here.

Boundary Conditions

The program was designed so that it will take any boundary condition. However, it is of interest to look at some of the standard boundary conditions encountered in continuous casting. These standard boundary conditions were used in getting the results presented later.

Center of Casting

This is treated as an insulating boundary condition

$$-k\frac{\partial T}{\partial r}\bigg|_{\text{center}} = 0$$

This is the natural boundary condition in finite element heat transfer analysis.

Top of the Casting

To "simulate" a refractory header used in D.C. casting, the top layer of elements is fixed at the pouring temperature [equation (4) with $T_\beta = T_{pouring}$].

Bottom Boundary

The bottom boundary is considered conducting. The total heat flux is by conduction and due to mass movement.

Circumferential Boundary

The circumferential boundary consists of mold, spray, and (in the case of steel) radiant zones.

Mold

The mold is considered to consist of a zone of good contact and a zone where an air gap forms. In the zone of good contact the total resistance to the heat flow (U_{good}) is the sum of the resistances due to a thin film of oil between the mold and the casting (U_{oil}) the thickness of the mold, and the interface between the mold and the mold cooling water:

$$U_{good} = U_{oil} + \frac{X_{mold}}{k_{mold}} + \frac{1}{h_{water}}$$

where X_{mold} is the thickness of the mold, k_{mold} is the conductivity of the mold material, and h_{water} is the heat transfer coefficient at the mold/water interface. As the solidified layer increases in thickness and cools down, it develops enough strength to withstand the metallostatic head, pulls away from the mold due to the solidification shrinkage, and an air gap forms between the mold and the solidified shell. The gap has a strong influence on the total heat transferred in the mold which in turn has an influence on gap formation. In the present analysis, the complex problem is treated by iteration (23). As will be seen later, this procedure gives results very close to what is obtained experimentally. The thermal resistance from the shell surface to the mold cooling water in the presence of an air gap is given by

$$U_{gap} = \frac{1}{\frac{k_{gap}}{\Delta g_{gap}} + \sigma\varepsilon(T^4-T_m^4)} + U_{good}$$

where U_{gap} is the total thermal resistance from the skin surface to the mold cooling water, k_{gap} is the thermal conductivity of the gas in the gap, Δg_{gap} is the thickness of the gap, T is the temperature of the surface of the skin and T_m is the temperature of the mold surface. Other terms are defined earlier.

Spray Zone

In the spray zone the heat transfer from the surface of casting to the spray water can be expressed by the relation

$$q = h_{spray}(T-T_{spray})$$

where T_{spray} is the temperature of spray and h_{spray} is the heat transfer coefficient in the spray. h_{spray} can be obtained from experiments such as those reported by Mizikar (17). Special techniques, such as delayed quench, may be simulated by varying the value of h_{spray}.

Radiant Cooling Zone

This is present only in continuous casting of steel. The heat transfer in this case can be given by

$$q = h_{rad}(T-T_\infty)$$

where the effective heat transfer coefficient in this zone, h_{rad}, is given by

$$h_{rad} = \sigma\varepsilon(T^2+T_\infty^2)(T+T_\infty)$$

Material Properties

The program has the capability for handling fixed and variable material properties. The variation of thermal conductivity and density with temperature have been extrapolated/interpolated from known values. The latent heat of solidification was included in the heat content of the material and distributed throughout the frequency range in proportion to the solid fraction formed. Both equilibrium and nonequilibrium solidification modes can be handled by the program. The convection in the liquid pool was handled by increas-

ing the thermal conductivity of the liquid metal as suggested by Mizikar (17).

Results

In order to test the accuracy of the present analysis, the results obtained from the analysis were compared with those reported in the literature for laboratory or industrial tests. Figures 2 and 3 show the comparison of the model predicted temperature profile with those reported by Adenis, Coats and Ragone (16) for magnesium D.C. casting. These investigators cast thermocouples on the surface, center and 2 inches from the surface of the casting and recorded the temperature profile for two mold diameters (15.8 and 9.5 cm.). The predicted profiles are found to be very close to those obtained experimentally.

Table 1 compares the sump depth reported by Adenis, Coats and Ragone for magnesium alloy AZ-80A D.C. castings with those obtained from the present analysis. Again, the agreement is found to be very good. Since the magnesium alloy has a very high thermal conductivity and is cast at very low speed, the axial heat conduction is very important in this case. This good agreement between the analysis and experimental values could not have been obtained if the axial heat conduction were ignored.

Figure 4 shows the comparison of the solidification profiles predicted by the model with those reported by Weinberg, et al.(13), from tests done at Western Canada Steel Company. These investigators have added radioactive tracers to the pool and determined the solidification profile from penetration of the tracer in the casting cross section. The agreement is very good between the shell thicknesses predicted from the analysis and the profiles obtained from industrial tests. Figure 5 and Figure 6 compares the predicted and measured (13) solidification profile for plain carbon steel and stainless steel slab. In measuring these profiles, the investigators had encountered problems in penetration of radioactive gold to the pool. Thus, the profile shown as measured may be slightly in error.

Table 2 compares the temperature of the skin on exit from the mold predicted by the model and those obtained experimentally by Gautier, et al. (19). These investigators have recorded the temperature of the casting on exit from the mold by channelling light with light pipes from the billet face to a two color pyrometer. They found that the temperature of the four faces of the billet fluctuated a great deal during the experiment. The values shown in the table are the average of the temperatures recorded at the four faces of the billet. The analysis is found to predict the temperature of the billet on exit from the mold with reasonable accuracy.

TABLE 1

Comparison of Predicted and Measured (16)

Sump Depth of Magnesium Alloy AZ80A Billet

Billet dia in	Casting Speed in/min	Mold length in	Calculated Sump depth in	Measured Sump depth in
16	2.1	9.5	18.17	14.0
16	2.1	16.5	18.44	18.5
16	3.0	16.5	21.60	22.8

TABLE 2

Comparison of Predicted and Measured (19)

Surface Temperature of Plain Carbon Steel Billet on Exit from Mold

Cast no	Steel Temp in Distributor °C	Withdrawal Speed cm/sec	Measured Billet Surface temp °C	Calculated Billet Surface temp °C
85 x 85 section				
42771	1520	4.9	1237	1231
13400	1503	5.1	1234	1224
13401	1503	5.9	1228	1241
13402	1536	5.1	1210	1287
105 x 105 section				
13761	1505	3.5	1093	1220
13763	1515	3.3	1089	1220
120 x 120 section				
42803	1508	3.0	1100	1213
13427	1545	2.7	1106	1241
13428	1546	3.2	1054	1259

Conclusions

The thermal analysis was found to be applicable to D.C. casting of nonferrous metals and the continuous casting of steel. The comparison of the results obtained from the model with the reported experimental values indicate that the agreement is very good. The analysis provides a powerful tool for the study of continuous casting process when used alone or along with a stress analysis model described in another paper.

Acknowledgements

The authors are grateful to the Office of Naval Research (Contract #N00014-67-A-0402-0003) and the ALCOA Foundation for contributing to the support of this project. The computations were performed at the Computer Center, University of Pittsburgh on the DEC-10 system.

References

1. J. Mathew and H. D. Brody, "Simulation of Thermal Stresses in Continuous Casting Using Finite Element Method," in these proceedings.

2. D. M. Lewis and J. Savage, Metallurgical Reviews, Vol. 1, Part 1 (1956) pp. 65-118.

3. J. Savage and W. H. Pritchard, Journal of the Iron and Steel Institute, Vol. 178 (1954), pp. 269-277.

4. L. H. W. Savage and R. T. Fowler, Journal of the Iron and Steel Institute, Vol. 173 (1953), pp. 119-128.

5. H. Krainer and B. Tarmann, Stahl u Eisen, Vol. 69 (1949), p. 813.

6. W. Weinreich, Steel Times, Vol. 189, No. 10 (Oct. 1970), pp. 735-739.

7. A. D. Akimenko, et al., Continuous Casting of Steel, p. 59, Iron and Steel Institute, London, 1962.

8. A. W. D. Hills, Proceedings of the Symposium on Chemical Engineering in the Metallurgical Industries, pp. 123-140, Institute of Chemical Engineers, London, 1963.

9. A. W. D. Hills, Journal of the Iron and Steel Institute, Vol. 203 (Jan. 1965), pp. 18-26.

10. A. W. D. Hills and M. R. Moore, Heat and Mass Transfer in Process Metallurgy, A. W. Hills (ed.), pp. 14-166, Institute of Mining and Metallurgy, London, 1967.

11. A. W. D. Hills, Trans. TMS-AIME, Vol. 246 (July 1969), pp. 1471-1479.

12. A. W. D. Hills and M. R. Moore, Transactions of TMS-AIME, Vol. 245 (July 1969), pp. 1480-1492.

13. J. Lait, J. K. Brimacombe and F. Weinberg, Continuous Casting, K. R. Olen (ed.), pp. 151-170, TMS-AIME, New York, 1973.

14. W. R. Irving, Journal of the Iron and Steel Institute, Vol. 205 (March 1967), pp. 271-277.

15. K. Cliff and R. J. Dain, Journal of the Iron and Steel Institute, Vol. 205 (March 1967), pp. 278-284.

16. Adenis, (D.J.P), K. H. Coats and D. V. Ragone, Journal of the Institute of Metals, Vol. 91, (1962-63), pp. 395-403.

17. E. A. Mizikar, Trans. TMS-AIME, Vol. 239, (Nov. 1969), pp. 1747-1753.

18. J. W. Donaldson and M. Hess, Continuous Processing and Process Control, T. R. Ingraham (ed.), Gordon and Beach Science Publishers, New York, 1968, pp. 299-300.

19. J. J. Gautier, Y. Morillon and J. Dumont-Fellow, Journal of the Iron and Steel Institute, Vol. 208 (Dec. 1970) pp. 1053-1059.

20. R. D. Pehlke, ASM Metals Engg Quarterly, Vol. 4, No. 2 (May 1964), p. 42.

21. L. Saroff, Continuous Casting, K. R. Olen (ed.), TMS-AIME, 1973.

22. O. C. Zienkiewicz, The Finite Element Method in Engineering, McGraw-Hill, New York, 1971.

23. J. Mathew and H. D. Brody, manuscript in preparation.

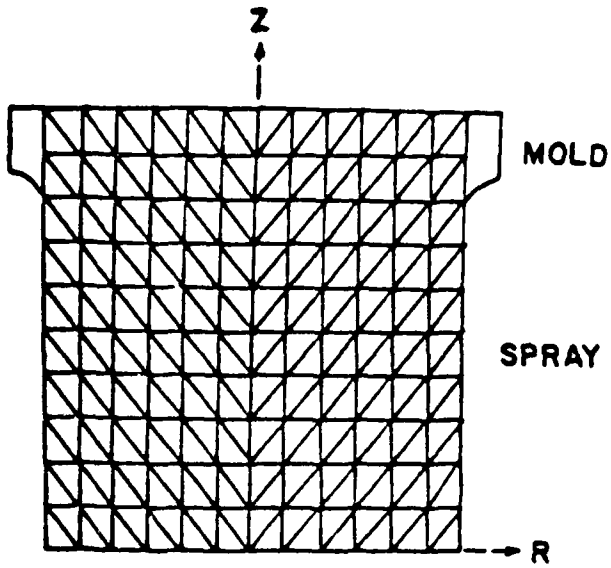

FIG 1a

Idealisation of the casting.

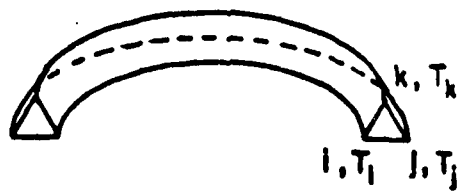

FIG 1b

Basic element used in the analysis i, j and k are the nodes and T_i, T_j and T_k are the nodal temperatures. Notice that nodes are circular here.

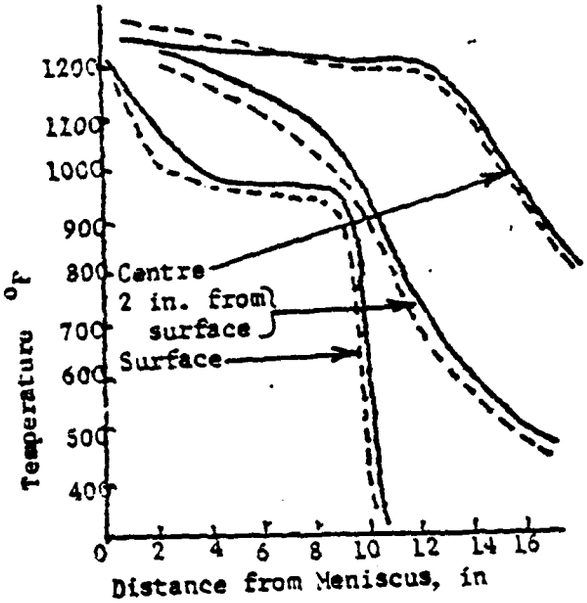

FIG 2

Comparison between calculated (——) and experimental (——) (16) temperature profiles for magnesium alloy AZ80A billet; billet of dia 16 in; mold length 9.5 in; casting speed 2.1 in/min.

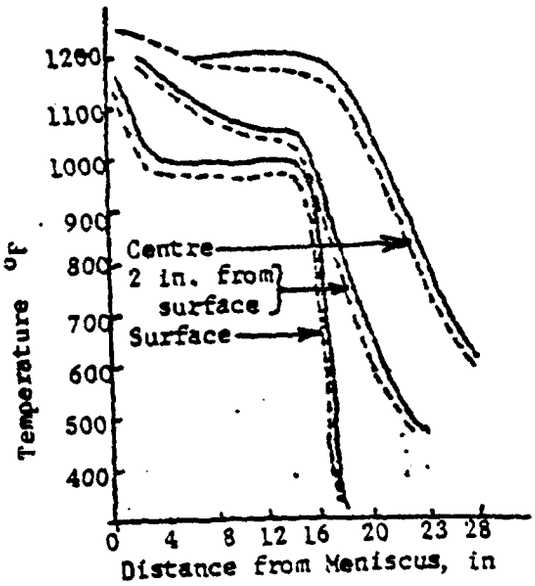

FIG 3

Comparison between calculated (——) and experimental (——) (16) temperature profile for magnesium alloy AX30A billet; billet dia 16 in; mold length 16.5 in; casting speed 2.1 in/min.

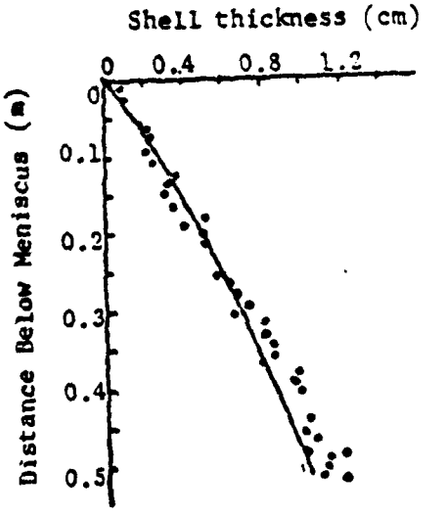

FIG 4

Comparison between calculated (——) and measured (•) (13) solidification profile 14x14 cm low carbon steel billet

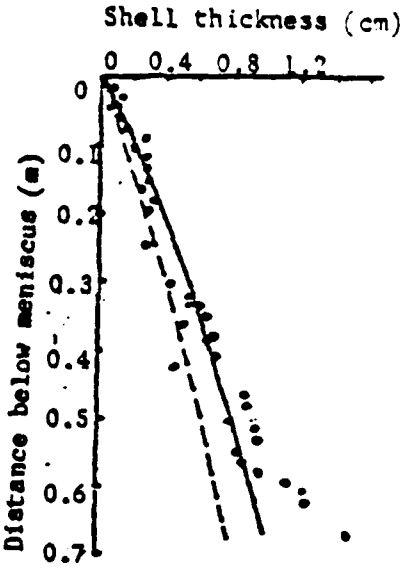

FIG 5

Comparison of the solidification profile obtained from the present analysis with those reported by Lait, et al. (13) for 13.3x13.3 cm low carbon steel billet
——analysis 3cm/sec;
---analysis 5cm/sec.

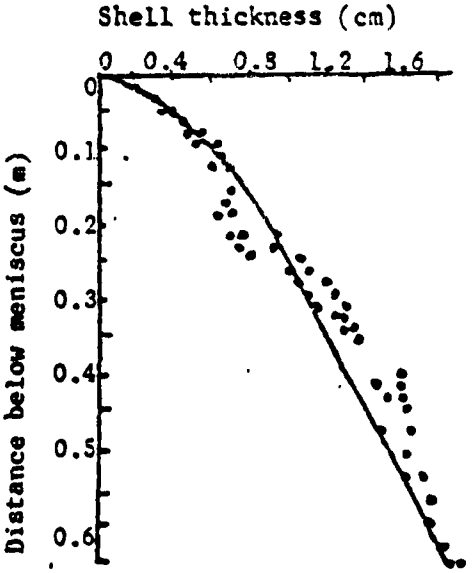

FIG 6

Comparison between the predicted (——) and measured (●) (13) solidification profile for stainless steel slab.

Presented at Conference on Computer Simulation for Materials Applications, Gaithersburg, MD, April 1976.

SIMULATION OF THERMAL STRESSES IN CONTINUOUS CASTING USING A FINITE ELEMENT METHOD

J. Mathew and H. D. Brody
Metallurgical and Materials Engineering
University of Pittsburgh

Abstract

This paper presents a three dimensional analysis of steady state thermal stresses developed in the continuous casting of cylindrical sections. The analysis takes into account the elastic, plastic and steady state creep deformations of the casting. It can take into account virtually all boundary conditions encountered in continuous casting (friction in the mold, metallostatic head, etc.) and is applicable to both ferrous and nonferrous continuous casting. The results from the analysis are compared to the published residual stress measurements made on Aluminum-12%Si alloy (A132). The model is very useful in understanding the influence of the operating parameters on the hot tearing and cold cracking of continuous castings.

Introduction

One of the continuing problems in the continuous casting of ferrous and nonferrous alloys is the incidence of cracking in the cast section. For example, aluminum alloys (2024 and 7075) are cast at extremely low speeds to avoid cracking. Higher casting rates would be desirable for reasons of productivity, surface finish, etc. The main cause for the formation of cracks is the development of thermal stresses in the casting during solidification and subsequent cooling. Hence, to understand the influence of operating parameters on the sensitivity of the casting to cracking, it is helpful to compute the thermal stresses developed in the casting. This paper describes a simulation program developed at the University of Pittsburgh to compute the thermal stresses in continuous casting. When used along with a heat transfer model of continuous casting (1), the analysis provides a powerful tool for understanding the origin of various thermal stress related defects in continuous casting.

The analysis presented in this paper is applicable to ferrous and nonferrous continuous castings of cylindrical section. It is a three dimensional axisymmetric analysis which takes into account the elastic, thermal, plastic and creep deformations of the material. The variation of mechanical properties of the material (elastic modulus, Poisson's ratio, coefficient of linear expansion, yield stress, plastic modulus and creep rate with temperature) can be taken into account in this analysis. The effect of body forces,

friction forces in the mold, metallostatic head, pinch roll pressure, and withdrawal forces can be considered. An automatic feature of the program is to set the thermal boundary condition in mold based on computing the position of formation and the width of the air gap. As the computation of stresses in the casting can be continued until the casting attains room temperature, the present analysis can be used to compute the residual stresses in the casting. The residual stresses can be measured experimentally, by techniques such as Sach's boring method. The simulation model can be used to predict the state of stress during solidification (which is very difficult to measure) after calibration with measurements on the casting of room temperature residual stresses.

In this paper, we shall briefly discuss the finite element analysis of thermal stresses in the casting. The results from the analysis are then compared to the residual stress measurements made on Aluminum Al32 alloy. The utility of the simulation model to study the hot tearing and cold cracking of the continuously cast sections will be indicated.

Analysis

The idealisation of the casting is similar to the one used for the heat transfer analysis (1). The basic element is a triangular ring element with three nodes. The displacement field (u) within this element is expressed in terms of nodal displacements (δ) by means of suitable interpolation functions $[N]$ (2):

$$(u) = [N]\ \{\delta\} \tag{1}$$

From the strain-displacement relations, the strain within the element can be computed as

$$\{\varepsilon\} = [B]\ \{\delta\} \tag{2}$$

where $\{\varepsilon\}$ is the column matrix of element strains and $[B]$ is the strain displacement matrix. From the stress-strain relations for the material we get the relation

$$\{\sigma\} = [D]\ (\{\varepsilon\} - \{\varepsilon_0\}) + \{\sigma_0\} \tag{3}$$

where $\{\sigma\}$ is the vector of element stresses. $[D]$ is the stress-strain matrix which depends on the properties of the material and the type of deformations considered. For the axisymmetric problem considered here, the strain and stress vectors are:

$$\{\varepsilon\} = \begin{Bmatrix} \varepsilon_z \\ \varepsilon_\theta \\ \varepsilon_r \\ \varepsilon_{rz} \end{Bmatrix} \quad \text{and} \quad \{\sigma\} = \begin{Bmatrix} \sigma_z \\ \sigma_\theta \\ \sigma_r \\ \tau_{rz} \end{Bmatrix} \tag{4}$$

For instance, if elastic analysis is carried out, the matrix $[D]$ can be derived from generalised Hooke's law. If plasticity or creep is to be considered, the analysis becomes nonlinear as the matrix $[D]$ now depends on the strain $\{\varepsilon\}$. The technique of handling plasticity and creep analysis will be discussed later. In equation (3), $\{\varepsilon_0\}$ is the initial strain matrix (thermal deformation is a very good example of the presence of an initial strain) and $\{\sigma_0\}$ is the initial stress matrix. The equivalent nodal forces that are to be applied at the nodes can be obtained by the application of the virtual work theorem.

$$[F]^e = [k]^e [\delta] + [F]^e_{\varepsilon_o} + [F]^e_{\sigma_o} + [F]^e_p \qquad (5)$$

$[F]^e$ are the element nodal forces, $[k]^e$ is the element stiffness matrix, $[F]^e_{\varepsilon_o}$, $[F]^e_{\sigma_o}$, and $[F]^e_p$ are the equivalent nodal forces due to initial strains, initial stresses, and body forces, respectively.

The equilibrium relations of the stress analysis are invoked in the derivation of the element stiffness matrix. The compatibility conditions are enforced by constraining the displacements at the nodes of the element to be unique. This is achieved by assembling the element stiffness matrices into a global stiffness matrix for the casting and defining a global matrix of nodal displacements. This gives

$$[K] [\bar{u}] = [F] \qquad (6)$$

Here $[K]$ is the global stiffness matrix, $[\bar{u}]$ is the global displacement matrix and $[F]$ is the force matrix for the casting. Equation (6) can be solved for the casting nodal displacements. The solution may be carried out by any of the standard methods like elimination methods or iteration methods. (Matrix inversion methods are not recommended as they involve considerable computer time.) In the present analysis, the Gaussian elimination method was used for the solution of the equations.

From the casting nodal displacements, the strains in the individual elements are computed using equation (2). The stresses in the element are computed from the strains using equation (3). From this, the principal stresses and strains are computed.

Handling of Plasticity, Creep and Thermal Strains

The handling of plastic, creep and thermal deformations in the analysis needs special attention. The total strain can be considered to consist of elastic, plastic, creep and thermal components.

$$\varepsilon_{total} = \varepsilon_{elastic} + \varepsilon_{thermal} + \varepsilon_{plastic} + \varepsilon_{creep} \qquad (7)$$

The elastic strains are related to the stresses by the Generalised Hooke's Law,

$$\varepsilon_{elastic} = \sigma/E \qquad (8)$$

where E is the modulus of elasticity of the material. The thermal deformations of the material affects only the dilatation and will not influence the shear strains. The initial strain due to the thermal strain thus become

$$[\varepsilon_o] = \begin{Bmatrix} \alpha\Delta T \\ \alpha\Delta T \\ \alpha\Delta T \\ 0 \end{Bmatrix} \qquad (9)$$

where α is the linear coefficient of expansion of the material and ΔT is the change of temperature from the stress free state.

The plastic strains are related only to the deviatoric stresses and they are not influenced by the hydrostatic stress. [Plastic strains cannot result in any volume

change.] The relation between the incremental plastic strains and the deviatoric stresses may be related by Prandtl Reuss relations

$$\Delta\varepsilon_r^p = \frac{1}{E_p}\ (2\sigma_r - \sigma_\theta - \sigma_z)$$

$$\Delta\varepsilon_\theta^p = \frac{1}{E_p}\ (2\sigma_\theta - \sigma_r - \sigma_z)$$

$$\Delta\varepsilon_z^p = \frac{1}{E_p}\ (2\sigma_z - \sigma_r - \sigma_\theta)$$

$$\Delta\varepsilon_{rz}^p = \frac{1}{E_p}\ (3\tau_{rz}) \qquad (10)$$

In equation (10), E_p is defined as

$$E_p = \frac{2\sigma_e}{\Delta\varepsilon_e^p}$$

where σ_e is the equivalent stress defined by

$$\sigma_e = \frac{1}{\sqrt{2}}\sqrt{(\sigma_r-\sigma_\theta)^2 + (\sigma_\theta-\sigma_z)^2 + (\sigma_r-\sigma_z)^2 + \tau_{rz}^2} \qquad (11)$$

and $\Delta\varepsilon_e^p$ is the incremental plastic strain. For the elements which have stresses above the yield stress of the material (determined by Mises' yield criterion), the matrix $[D]$ in equation (3) is modified into a plastic stress-strain matrix $[D_p]$. In order to conserve computer time, the element stiffness matrix is left unaltered. This can be achieved by writing

$$[D_p] = [D] + [D']$$

where $[D_p]$ is the actual plastic stress-strain matrix, $[D]$ is the elastic stress-strain matrix and $[D']$ is the difference between $[D_p]$ and $[D]$. The relation between stress and strain can be written as

$$\{\sigma\} = [D_p]\{\varepsilon\}$$

$$= [D]\{\varepsilon\} + [D']\{\varepsilon\}$$

$$= [D]\,[\{\varepsilon\} + \{\varepsilon_0'\}] \qquad (12)$$

Thus, the plastic strains result in initial strain $\{\varepsilon_0'\}$ which do not alter the stiffness matrix of the element. Only the force vector is affected. The stiffness matrix may be triangularised after the assembly process. The subsequent solutions will affect only the back substitution process. This method saves considerable amount of computer time as in the Gaussian elimination method triangularisation of the matrix consumes most of the computer time.

The creep strains are handled in an identical manner. The creep rate is related to the equivalent stress by the creep law of the material. From the creep strain and equivalent stresses, the individual components of strain are computed using equation(10). The creep strains are handled as initial strains and the equivalent nodal forces are

computed. The new casting nodal displacements are computed by back substitution.

Boundary Conditions

The simulation program was designed to handle the widest range of boundary conditions. The boundary conditions used to obtain the results presented later are discussed in this section.

Bottom of the Casting

The boundary is considered to be fixed axially; but free to move radially.

Center of Casting

The casting is fixed radially, but is free to move axially.

Top of the Casting

Above a certain temperature a liquid plus solid mixture behaves like a liquid and below that temperature the mixture behaves like a solid. This temperature is termed a coherency temperature. To account for the mushy zone in the casting, the elements which are above the coherency temperature are removed and on the surface of the resulting boundary the metallostatic head is applied.

Circumferential Boundary

This consists of mold zone and the spray. In the spray zone, the boundary is free. In the mold the elements may or may not be constrained radially depending on whether an air gap is present. In the program, the mold boundary condition may be specified or it may be generated by the program itself. In the latter case the casting surface is allowed to move inward or outward except that the mold diameter is considered a limiting dimension.

Results

Before discussing the application of the analysis to continuous casting, two methods of checking the accuracy of the analysis are discussed. First, the accuracy of the displacement field was checked by applying the analysis to certain ideal cases where closed form analytical solutions are available in the literature. Both thermal stress and creep analyses were checked. The accuracy of the model when applied to continuous casting was checked by comparing the model predicted stress values to published residual stress measurements made on continuous casting.

The thermal stress analysis model (elastic) was checked by applying the analysis of a hollow thick cylinder with a steady state temperature distribution. The elastic thermal stresses developed in the cylinder were computed and compared to the results of an analytical solution to this problem given by Johnson and Mellor (3). Figure 1 compares the model predicted stress values with the exact solution for a hollow cylinder of inside and outside radii of 10 and 20 inches, respectively, with the inner surface maintained at 100°C and outer surface maintained at 200°C. The agreement is found to be very good between the analytical results and the exact solution.

The steady state creep analysis was checked by applying the model to the case of a hollow thick cylinder with a uniform pressure inside the cylinder. The elastic and steady state creep stresses have been calculated by Odquist (4) for this case when the steady state creep rate is given by the law

$$\dot{\epsilon} = 6.4 \times 10^{-18} \sigma_e^{4.4}$$

where $\dot{\epsilon}$ is the creep rate and σ_e is the equivalent stress. The model was applied to the case of a cylinder of inner radius 0.16" and outer radius 0.25" with a uniform inner pressure of 365 psi. The elastic and creep stresses are shown in Figure 2. Again, note that the agreement between the exact solution and the model predicted values is very good.

Using Sachs boring technique, Roth, et al. (5) measured the residual stresses in 6.5 inch and 5.7 inch diameter Al-12%Si alloy ingots. The ingots were cast at speeds of 8.95 and 17.1 in/min. The 6.5 inch diameter ingot was found to have a residual longitudinal tensile stress of 26,000 psi at the axis when cast at these rates. This was found to decrease toward the surface and changed to compressive stresses 1.14 inches below the surface, the stresses was -14,000 to -18,000 psi. Roth concluded that for the two ingot sizes tested, the rate of casting had no marked effect on the room temperature residual stresses. But the cracking tendency was found to increase with the increase in casting speed.

The present analysis was used to simulate the casting of Al32 alloy ingots 6.5 inches in diameter. The axial stresses obtained from the present analysis are shown in Table 1-2 for casting speeds of 8.95 in/min and 17.1 in/min. The results are summarized in Table 3 along with the experimental results obtained by Roth, et al. Notice that the agreement is fairly good between the model predicted residual stresses and those obtained experimentally. The present analysis also predicts quite accurately the reversal of the stresses from tensile to compressive near the surface.

The cracking generally originates near the end of solidification and hence the stresses during the solidification of the alloy are of interest. To date these have not been obtained experimentally. Analyses of type presented here are necessary to estimate stresses in the casting during solidification.

Since the temperature changes from the top to bottom of the casting, the absolute stresses as given in Tables 1 and 2 do not give much insight as to the severity of the stress level. Thus, the stress values were normalised by dividing by the yield stress of the material at the temperature of the element. The maximum normalised stress (maximum of hoop, radial or axial stress) at different levels of continuously cast Al32 is given in Tables 4 and 5. (The temperatures at the points where the stress is computed are tabulated below the stress values.) Notice that for the casting conditions simulated here, the maximum normalised stress appears just at the solidification front. The value

TABLE 1

Computed Axial Stresses in a Cylindrical Al-12%Si Alloy (A132) Casting of Diameter 6.5 inches Cast at 8.95 in/min

PITT, CONTINUOUS CASTING THERMAL & STRESS SIMULATION (PCCTSS-VERSION,,2A)
A132 (CASTING SPEED=8.95 IN/MIN) G=16.4 CM DIA
14-APR-76 16:34
DSI= 0.186E+00

ROW	AVERAGE AXIAL STRESSES AFTER ITERATION NO: 197						
1	-362.	55.	474.				
2	1979.	-1701.	-2094.	-52.	1435.	1413.	1275.
3	28.	-788.	-1744.	-1159.	2906.	3997.	6714.
4	-3608.	-1892.	-1370.	194.	6348.	11161.	14734.
5	-6330.	-3173.	-1148.	1824.	9369.	16943.	19703.
6	-8913.	-4195.	-709.	3478.	12181.	20896.	24574.
7	-10818.	-4968.	-457.	4707.	14266.	23806.	28119.
8	-11925.	-5445.	-328.	5388.	15512.	25698.	30537.
9	-11931.	-5598.	-450.	5393.	15700.	26141.	31368.
10	-11632.	-5557.	-548.	5232.	15484.	25824.	30986.
11	-12067.	-5596.	-385.	5486.	15794.	26188.	31260.
12	-12676.	-5765.	-239.	5848.	16339.	26939.	32223.
13	-12955.	-5905.	-218.	6023.	16672.	27450.	32901.
14	-13168.	-5997.	-191.	6159.	16911.	27791.	33324.
15	-13316.	-6086.	-241.	6221.	17151.	28210.	33441.
16	-12416.	-5469.	-300.	5200.	15817.	26748.	29738.

TABLE 2

Computed Axial Stresses in a Cylindrical Al-12%Si Alloy (A132) Casting of Diameter 6.5 inches Cast at 17.1 in/min

PITT, CONTINUOUS CASTING THERMAL & STRESS SIMULATION (PCCTSS-VERSION,,2A)
A132 (CASTING SPEED=17.1 IN/MIN) G=16.4 CM DIA
14-Apr-76 14:43
DSI= 0.584E+00

ROW	AVERAGE AXIAL STRESSES AFTER ITERATION NO: 203						
1	-3.						
2	1356.	-1590.					
3	3189.	500.	-4225.	-1019.			
4	844.	2326.	-716.	-1747.	-3054.		
5	-2140.	1667.	1274.	213.	817.	-3237.	2969.
6	-5482.	2525.	2155.	1637.	1604.	2782.	-4867.
7	-9009.	2232.	3183.	4072.	3391.	5139.	3536.
8	-11679.	1556.	3804.	5851.	6272.	7757.	5252.
9	-13238.	958.	4204.	6697.	7963.	10052.	7733.
10	-14031.	547.	4542.	7054.	8840.	11314.	9234.
11	-15204.	322.	5185.	7564.	9700.	12393.	10296.
12	-16275.	-115.	5752.	8123.	10662.	13602.	11580.
13	-16755.	-618.	6068.	8388.	11346.	14559.	12638.
14	-17082.	-1297.	6343.	8715.	12020.	15474.	13635.
15	-17472.	-2554.	6529.	9650.	13156.	16824.	15233.
16	-18287.	-5358.	6259.	12041.	16196.	20207.	19065.

TABLE 3

Comparison of Axial Residual Stresses Predicted by Model with Values Measured by Roth, et al. (5) for a 6.5 inch diameter A132 Alloy Ingot

Casting Speed (in/min)	Tensile Stress at Axis (psi)		Compressive Stress 0.2" from Surface (psi)		Distance from Surface for Reversal of Stress (inches)	
	Model	Experimental	Model	Experimental	Model	Experimental
8.95	33,000	26,000	13,000	14-18,000	1.14	1.14
17.10	20,000	26,000	18,000	14-18,000	0.95	1.14

TABLE 4

Computed Maximum Normalised Stress and Temperature Distribution in an A132 Alloy, 6.5 in. dia. Casting Poured at 8.95 in/min

PITT. CONTINUOUS CASTING THERMAL & STRESS SIMULATION (PCCTSS-VERSION..2A)
A132 (CASTING SPEED=8.95 IN/MIN) 6)16.4 CM DIA
14-APR-76 16:34

MAXIMUM NORMALISED STRESS

1	0.652	0.821	1.548				
2	0.428	-0.043	-0.093	0.443	1.213	1.860	2.151
3	0.129	0.186	0.332	0.493	0.750	0.945	1.689
4	0.011	0.132	0.293	0.470	0.745	1.303	1.829
5	0.035	0.164	0.324	0.490	0.704	1.218	1.479
6	0.042	0.187	0.347	0.501	0.687	1.166	1.406
7	0.053	0.207	0.370	0.514	0.687	1.149	1.378
8	0.053	0.215	0.380	0.524	0.697	1.166	1.399
9	0.053	0.208	0.368	0.508	0.685	1.150	1.393
10	0.072	0.211	0.356	0.484	0.652	1.096	1.328
11	0.072	0.216	0.360	0.481	0.643	1.072	1.291
12	0.062	0.214	0.363	0.489	0.659	1.088	1.309
13	0.065	0.217	0.367	0.493	0.669	1.104	1.330
14	0.065	0.219	0.370	0.497	0.677	1.118	1.344
15	0.061	0.216	0.369	0.503	0.686	1.130	1.350
16	0.062	0.209	0.328	0.442	0.724	1.200	1.386

TEMPERATURE DISTRIBUTION

1	468.	529.	581.				
2	249.	318.	378.	430.	469.	497.	515.
3	155.	204.	249.	288.	319.	342.	356.
4	140.	170.	200.	227.	249.	265.	274.
5	128.	149.	170.	189.	205.	216.	223.
6	119.	133.	148.	161.	171.	179.	184.
7	112.	122.	131.	140.	147.	152.	155.
8	109.	116.	122.	127.	132.	135.	137.
9	103.	109.	115.	120.	123.	126.	127.
10	88.	96.	102.	107.	112.	115.	116.
11	78.	84.	90.	95.	99.	102.	104.
12	76.	80.	85.	89.	92.	94.	96.
13	75.	78.	82.	85.	88.	90.	91.
14	74.	77.	80.	83.	85.	87.	88.
15	74.	76.	79.	82.	84.	86.	86.
16	73.	76.	79.	81.	83.	85.	86.

TABLE 5

Computed Maximum Normalised Stress and Temperature Distrubution in an A132 Alloy, 6.5 in. dia. Casting Poured at 17.1 in/min

PITT. CONTINUOUS CASTING THERMAL & STRESS SIMULATION (PCCTSS-VERSION,.2A)
A132 (CASTING SPEED=17.1 IN/MIN) G;16.4 CM DIA
14-Apr-76 14:43

MAXIMUM NORMALISED STRESS

1	0.502						
2	0.871	-0.858					
3	0.523	0.373	-3.036	-1.678			
4	0.079	0.459	0.107	-1.352	-5.090		
5	0.003	0.189	0.354	0.199	0.859	-4.008	4.971
6	0.011	0.236	0.323	0.529	0.767	1.313	-2.534
7	0.020	0.187	0.359	0.609	0.990	1.845	1.387
8	0.037	0.199	0.341	0.530	0.781	1.156	1.036
9	0.045	0.207	0.349	0.459	0.635	0.863	0.820
10	0.068	0.216	0.401	0.400	0.540	0.728	0.665
11	0.072	0.226	0.453	0.370	0.502	0.672	0.591
12	0.053	0.227	0.498	0.370	0.500	0.657	0.581
13	0.064	0.232	0.532	0.365	0.506	0.662	0.588
14	0.074	0.239	0.540	0.368	0.518	0.677	0.607
15	0.090	0.241	0.500	0.403	0.555	0.717	0.659
16	0.116	0.276	0.449	0.528	0.691	0.854	0.809

TEMPERATURE DISTRIBUTION

1	591.						
2	396.	524.					
3	251.	375.	488.	572.			
4	212.	301.	393.	485.	559.		
5	186.	254.	327.	402.	476.	536.	564.
6	167.	220.	274.	328.	378.	422.	449.
7	152.	193.	233.	271.	303.	328.	343.
8	142.	173.	203.	231.	255.	272.	281.
9	130.	156.	181.	202.	220.	233.	240.
10	111.	135.	157.	176.	191.	202.	208.
11	96.	117.	136.	152.	165.	175.	180.
12	90.	106.	121.	134.	145.	152.	157.
13	86.	98.	110.	121.	130.	136.	139.
14	83.	93.	103.	111.	119.	124.	127.
15	81.	89.	97.	105.	111.	115.	118.
16	79.	87.	94.	100.	106.	110.	112.

is 2.15 for the ingot cast at 8.95 in/min and 4.97 for the ingot cast at 17.1 in/min. This indicates that the ingot cast at 17.1 in/min is more prone to hot tearing than the one cast at 8.95 in/min (as observed by Roth). Since the maximum stress appears at the axis of the casting, the crack, if formed, will be axially symmetric (ghost or star cracks).

Summary

The analysis presented in this paper is very useful in studying the effect of operating parameters on continuous casting. As the stresses in the solidification range as well as down to room temperature can be obtained, it can be used to simulate both hot tearing and cold cracking of the casting. The analysis gives the principal stresses, maximum normalised stresses at different points in the casting, plastic strain in the element and final diameter of the casting after cooling. This information is sufficient to arrive at a criterion for hot or cold cracking of the casting. It is applicable to any alloy (aluminum D.C. casting as well as continuous casting of steel). The accuracy of the analysis can be checked by room temperature residual stress measurements. Mold length, heat transfer in the secondary cooling zone, superheat, etc. are very important parameters which influence the hot tearing tendency of the material.

The agreement between the hot tearing tendency of castings as predicted from the present model and the practical experience in the D.C. casting of Aluminum 6063, 5084 and 2014 alloys are found to be very good. The model is being used at present for a parametric study of the hot tearing in continuously cast sections.

Acknowledgements

The authors are grateful to the Office of Naval Research (Contract #N00014-67-A-0402-0003) and the ALCOA Foundation for contributing to the support of this project. The computations were performed at the Computer Center, University of Pittsburgh on the DEC-10 system.

References

1. J. Mathew and H. D. Brody, "Analysis of Heat Transfer in Continuous Casting Using Finite Element Method," elsewhere in this proceeding.

2. O. C. Zienkiewicz, The Finite Element Method in Engineering Science, McGraw-Hill, London, 1974.

3. W. Johnson and P. B. Mellor, Engineering Plasticity, Van Nostrand Reinhold, New York, 1973.

4. F. K. G. Odquist and J. Hutt, Kriechfestigkeit Metallischer Werk Stoffe, Springer-Verlag, Berlin 1962.

5. A. Roth, et al., Aluminum, Vol. 24, 1942, p. 206.

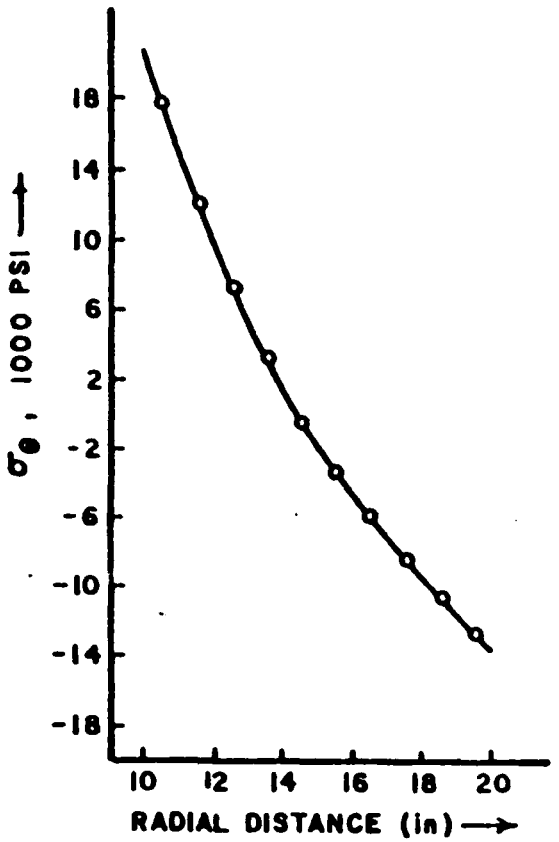

FIG 1a

Comparison between computed and exact (3) hoop stresses in a thick cylinder with steady state temperature distribution.

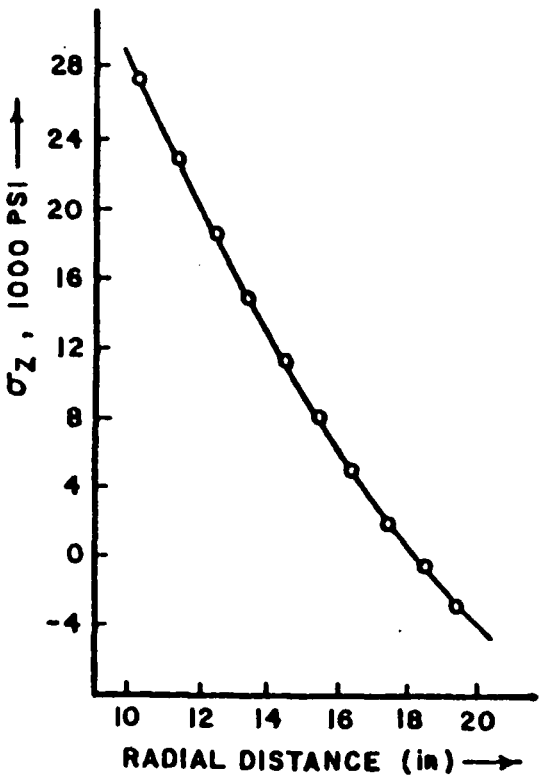

FIG 1b

Comparison between computed and exact (3) axial stresses in a thick cylinder with steady state temperature distribution.

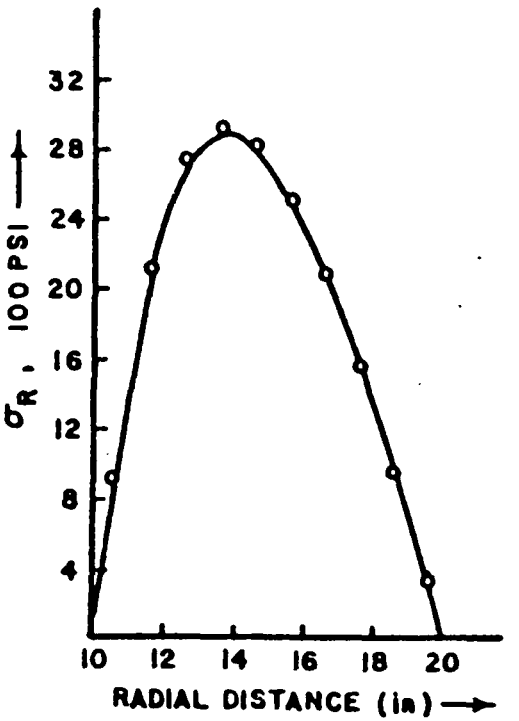

FIG 1c

Comparison between computed and exact (3) radial stresses in a thick cylinder with steady state temperature distribution.

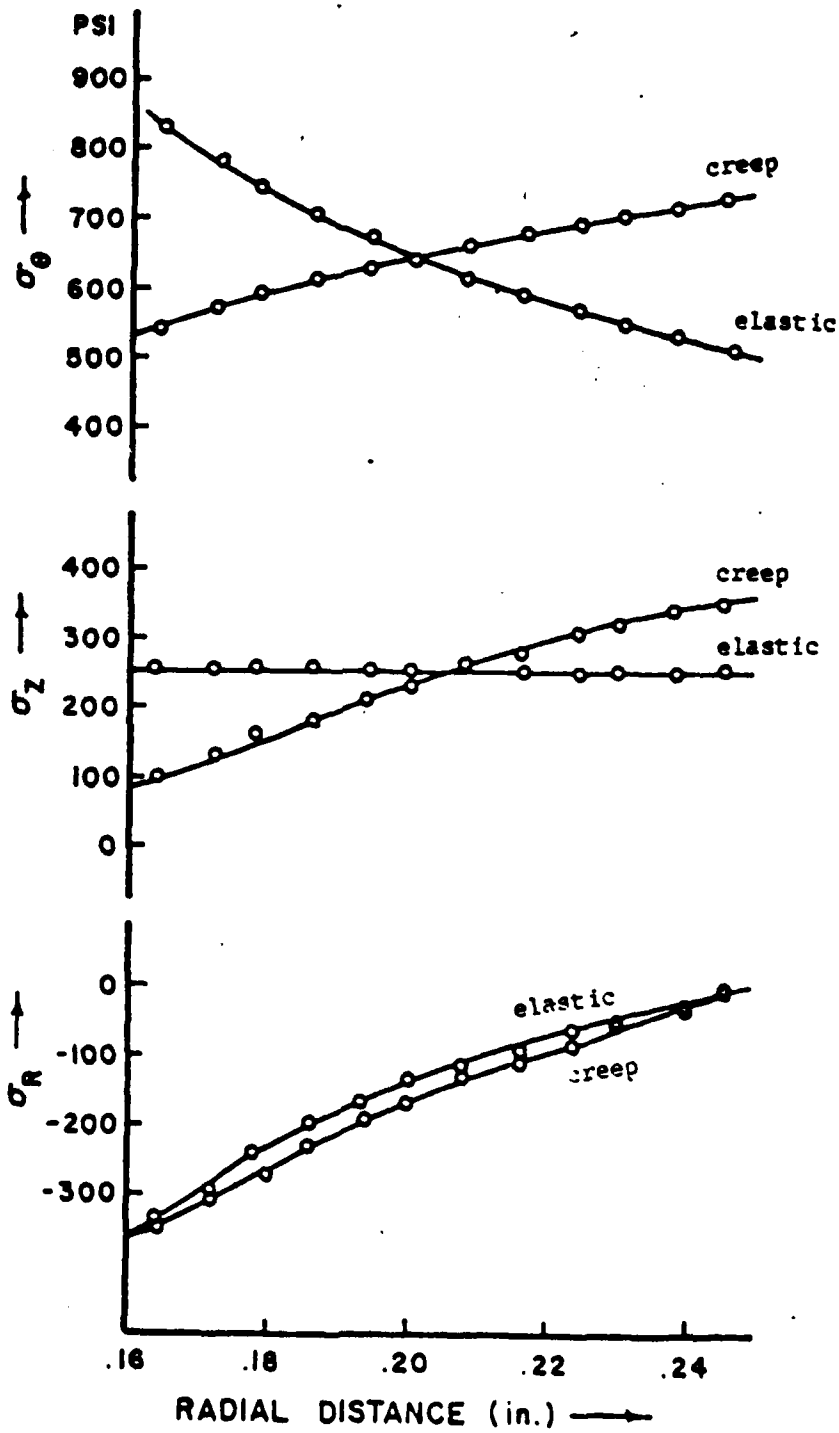

FIG 2

Comparison between the computed and exact (4) hoop (σ_θ), axial (σ_z) and radial (σ_r) stresses in a hollow cylinder with uniform internal pressure.

SECURITY CLASSIFICATION OF THIS PAGE (When Data Entered)

REPORT DOCUMENTATION PAGE		READ INSTRUCTIONS BEFORE COMPLETING FORM
1. REPORT NUMBER	2. GOVT ACCESSION NO.	3. RECIPIENT'S CATALOG NUMBER
4. TITLE (and Subtitle) Effect of Solute Redistribution on the Structure and Properties of Cast Alloys		5. TYPE OF REPORT & PERIOD COVERED Technical Report
		6. PERFORMING ORG. REPORT NUMBER SETEC-MME-76-030
7. AUTHOR(s) J. Mathew, S. A. David, K. Y. Lin and H. D. Brody		8. CONTRACT OR GRANT NUMBER(s) N0014-75-C-0800
9. PERFORMING ORGANIZATION NAME AND ADDRESS Metallurgical and Materials Engineering University of Pittsburgh Pittsburgh, Pennsylvania 15261		10. PROGRAM ELEMENT, PROJECT, TASK AREA & WORK UNIT NUMBERS
11. CONTROLLING OFFICE NAME AND ADDRESS Metallurgy Program, Office of Naval Research 800 N. Quincy Arlington, Virginia 22217		12. REPORT DATE August 1976
		13. NUMBER OF PAGES 31
14. MONITORING AGENCY NAME & ADDRESS(if different from Controlling Office)		15. SECURITY CLASS. (of this report) Unclassified
		15a. DECLASSIFICATION/DOWNGRADING SCHEDULE

16. DISTRIBUTION STATEMENT (of this Report)

Unlimited

DISTRIBUTION ... Approved ...

17. DISTRIBUTION STATEMENT (of the abstract entered in Block 20, if different from Report)

18. SUPPLEMENTARY NOTES

Report includes reprints of papers (2) published in vol. 20 of Nuclear Metallurgy as the Proceedings of the "Conference on Computer Simulation for Materials Applications," at Gaithersburg, Md., April 1976.

19. KEY WORDS (Continue on reverse side if necessary and identify by block number)

solidification
composites
eutectics
continuous casting
computer analyses
casting

20. ABSTRACT (Continue on reverse side if necessary and identify by block number)

This report summarizes work on composite and alloy solidification presently conducted under the ONR contract and includes two papers on the simulation of heat flow and thermal stresses in continuous casting presented at the "Conference on Computer Simulation for Materials Applications" in Gaithersburg, Md. in April 1976.

A final element analysis of heat transfer in continuous casting is presented in the first paper. The steady state conditions of the solidifica-

DD FORM 1 JAN 73 1473 EDITION OF 1 NOV 65 IS OBSOLETE
S/N 0102-014-6601

402 241

SECURITY CLASSIFICATION OF THIS PAGE (When Data Entered)

tion of a cylindrical alloy ingot are simulated. The analysis takes into account both radial and axial heat conduction and the variation of alloy properties with temperature. The analysis has the versatility to simulate any casting configuration as the program has the capability to treat any arbitrary boundary conditions. In the mold region, where an air gap generally forms, the position of gap formation, the size of the gap and the heat transfer through the gap by conduction and radiation are computed. Values predicted by the model are in close agreement with published laboratory and industrial data.

The second paper presents a three dimensional analysis of steady state thermal stresses developed in the continuous casting of cylindrical sections. The analysis takes into account the elastic, plastic and steady state creep deformations of the casting. It can take into account virtually all boundary conditions encountered in continuous casting (friction in the mold, metallostatic head, etc.) and is applicable to both ferrous and nonferrous continuous casting. The results from the analysis are compared to the published residual stress measurements made on aluminum-12% silicon alloy (A132). The model is very useful in understanding the influence of the operating parameters on the hot tearing and cold cracking of continuous castings.